

MODELLING OF X-RAY VOLUME EXCITATION OF THE XLO GAIN MEDIUM USING FLASH

P. Manwani*, N. Majernik, B. Naranjo, J. B. Rosenzweig, UCLA, Los Angeles, CA, USA
E. Galtier, A. Halavanau, C. Pellegrini, SLAC, Menlo Park, CA, USA

Abstract

Plasma dynamics and crater formation of laser excited volumes in solids is a complex process due to thermalization, shockwave formation, varying absorption mechanisms, and a wide range of relevant physics timescales. The properties and interaction of such laser-matter systems can be modeled using an equation of state and opacity based multi-temperature treatment of plasma using a radiation hydrodynamics code. Here, we use FLASH, an adaptive mesh radiation-hydrodynamics code, to simulate the plasma expansion following after the initial energy deposition and thermalization of the column, to benchmark the results of experiments undertaken at UCLA on optical laser ablation. These computational results help develop a quantitative understanding of the material excitation process and enable the optimization of the gain medium delivery system for the x-ray laser oscillator project [1].

INTRODUCTION

The x-ray laser oscillator, termed XLO [1], is a project at the Stanford Linear Accelerator Facility (SLAC) to induce population inversion of the electrons in copper using an x-ray free electron laser (XFEL) to deliver pump pulses to enable stimulated emission in the at the K_α line of the gain medium. The proposed gain medium is a liquid jet of copper sulphate or a solid copper foil. This gain medium needs to be rapidly replaced so each subsequent pulse, spaced at ~ 30 ns, has fresh material [2, 3]. The required speed of the target depends on the crater geometry left by the x-ray pulse and simulations using FLASH (adaptive mesh hydrodynamic code solver) [4, 5] will be used to understand the laser plasma interaction and resulting ablation. We use this code to study the plasma evolution as particle-in-cell codes are computationally intensive at these densities. The FLASH code supports a tabulated equation of state (EOS) and opacity based multi-temperature model for plasmas. This is important as the thermodynamic properties of materials at high temperatures and pressure cannot be modelled using a power law. Specifically, we use the tabulated EOS and radiative opacity from the PROPACIOS [6] database that calculates the ionization using the Saha model [7] which yields the ionization degree of a plasma at a equilibrium temperature. There are two kinds of interaction regimes that we want to investigate using this code: optical and x-ray ablation. FLASH has capabilities to model both types of interactions, albeit with some assumptions on the initial conditions; these will be described below. Experiments were performed to

optically ablate copper foils to benchmark the FLASH simulations and these results are presented in the context of the XLO project.

OPTICAL ABLATION

During the development of the sample delivery system, it is challenging to get access to XFEL pulses for iterative testing. Instead, we turn to the use of an optical laser to approximate certain aspects of the laser-target interaction. Two elements in particular are of the greatest interest for target development: characterizing the longitudinal oscillations caused by the ablation of the target and the longevity of the target as more and more damage is done. The constraints on the allowed oscillation ($<30 \mu\text{m}$) and target lifetime (\sim hours) are discussed in [3].

Since the optical laser cannot be focused as tightly as an x-ray pulse (10s of μm vs 100s of nm) and since the interaction is largely at the surface, rather than a volume interaction, the expected impulse from the optical laser is a worst case scenario. Using a Nd:YAG laser (max energy, 500 mJ/pulse) and a short focal length lens (100 mm), the energy of the laser pulse was reduced until the focused beam was barely able to create a hole through the 25 μm thick foil. Then, the spatial profile of the focus was measured using a CCD, the temporal profile was measured with a fast photodiode, and the energy was recorded using a pyroelectric laser energy meter. These measured parameters informed the simulation settings, detailed in Table 1. The ablated foils were imaged using a scanning electron microscope (SEM) with the results are shown in Fig. 1. These benchmarked, optical laser simulations will be compared to simulations of the XFEL-target interaction to confirm that the impulse and crater size of the optical case are, indeed, representative of a worst case scenario. Finally, the target will be exposed to a series of optical laser shots; if the target satisfies both the longevity and oscillation requirements (characterized by laser Doppler vibrometry) we may be confident that it will perform well when installed on an XFEL beamline.

Table 1: Laser Parameters

Parameter	Value	Unit
Laser energy, E_l	77	mJ
Laser wavelength, λ_l	1064	nm
Pulse duration (FWHM)	20	ns
Beam diameter (before lens)	6	mm
Focal length (lens)	100	mm
Beam waist ($1/e^2$)	35	μm

* pkmanwani@gmail.com

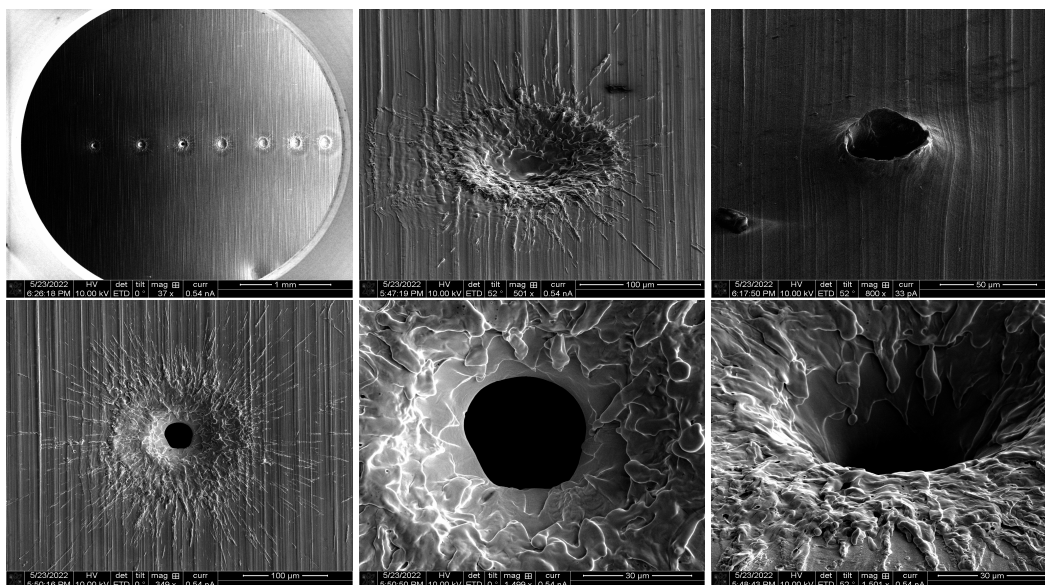


Figure 1: SEM images of optical laser induced craters to benchmark simulation results. **Top left** A sequence of optical laser shots were taken on a copper foil, varying the longitudinal location relative to the focus. Shots upstream and downstream of the focus are less effective at penetrating through the foil. **Top center** A shot taken slightly away from the laser waist. Although material has been ablated and ejected, the foil was not penetrated. **Top right** The backside of the foil at a crater formed near the laser focus. The copper has been deformed backwards. **Bottom row** A series of images of the same crater, formed near the laser focus, at different SEM magnifications and tilt angles.

Table 2: Simulation Parameters for optical ablation

Parameter	Value	Unit
Simulation window (r,z),	(60, 60)	μm
Grid cells	(80, 80)	-
Mesh refinement level	1	-
Target temperature	300	K
Target width	20	μm
Target melting point (artificial)	1,358	K
CFL	0.05	-
Number of rays (laser)	10,000	-

The simulations were performed using the above described laser and simulation parameters shown in Table 3. The current implementation of FLASH treats the laser beam in the geometric optics approximation. Beams are simulated as of rays that are traced through the domain based on the local refractive index, which is updated each timestep. The energy deposition of the laser pulse is modelled in FLASH based on the inverse bremsstrahlung power in each cell and is dependent on the local electron number density and local electron temperature gradient. The simulation was run for 60 ns, over which time a crater is created. FLASH considers the solid target as a high density gas and this gas diffuses at these timescales. This diffusion was artificially stopped by stopping the hydrodynamic evolution of the gas below the melting point. A plasma plume is created initially by the laser and it continues to grow as material is ejected out. The energy deposition typically occurs at the edge of the

foil and interacts with the plasma plume. The high density of the plasma reflects the bulk of the laser rays and the results in the electron temperature attaining its highest point away from the surface. The crater formed at the end of the simulation is shown in Fig. 2. The crater shape and size resemble the craters observed in the experiment but the laser does not penetrate the copper foil. This might be due to several reasons: the timescales of crater formation might be larger than the timescales of the simulation; the energy deposition model in FLASH might be missing some relevant physics; and artificially stopping the diffusion of the solid might stop the pressure shocks from deforming the material and propagating through the target. A possible solution to the latter problem would be to use the quotidian equation of state (QEOS) [8] to simulate the material characteristics of the solid, which achieves negligible total pressures for cold solids by allowing the electron pressure to be negative [9].

X-RAY ABLATION

In the XLO project, the gain medium will be ablated by x-ray pulses. In this case, the x-rays are absorbed volumetrically, and create energetic electrons due to photoionization and Auger decay. Auger transitions are more probable in lighter elements, while x-ray yield is dominant in heavier elements. Copper has an x-ray yield of 40% while the rest of the energy is contained in the Auger electrons. These Auger electrons collide with other electrons and ions and thermalize to create a high temperature plasma column. Solving for the electron temperature analytically is challenging as all ionization levels and cross sections need to be considered.

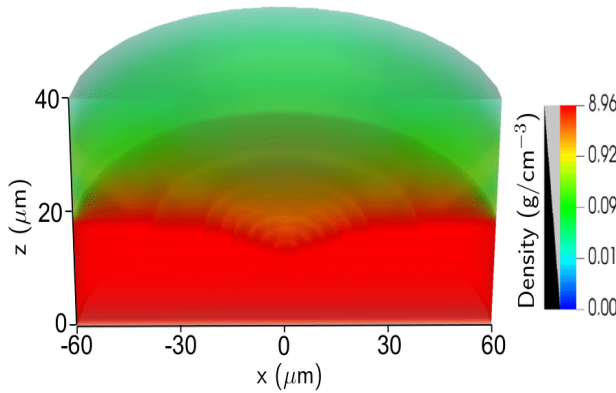


Figure 2: Simulation snapshot showing the crater formed in the solid copper foil 60 ns after the optical laser induced surface ablation.

The timescales for temperature equilibration vary for the ion and electrons and is on the order of a tens of ps for the ions compared to tens of fs for the electrons if we use the Landau Spitzer model for weakly coupled and fully ionized plasmas [10]. The pulse length of the XFEL beam at SLAC is 20 fs (FWHM) and the laser target interaction occurs at short time scales compared to the electron ion equilibration time. Therefore, a two temperature treatment is necessary to simulate the physics. X-ray ablation cannot be simulated directly in FLASH, but the two temperature plasma can be simulated. The physical dimensions of the two temperature plasma column can be found by using the attenuation length of the XFEL pulse while its diameter can be assumed to be the width of the XFEL pulse.

Table 3: Simulation Parameters for x-ray ablation

Parameter	Value	Unit
Simulation window (r, z)	(40, 30)	μm
Grid cells	(400, 400)	-
Mesh refinement level	2	-
Target temperature	300	K
Target width	20	μm
Plasma column electron temperature	1.2×10^6	K
Plasma column ion temperature	300	K
Plasma column width	100	nm
Attenuation length	4	μm
CFL	0.1	-

We assume that the ion temperature does not change and consider the processes after the initial electron-electron equilibration. The electron temperature of the plasma column was determined by considering the dominant processes of photoionization and Auger decay and an upper limit for the initial condition was estimated to be around 100 eV. The attenuation length of copper at 9 keV is about 4 μm and the

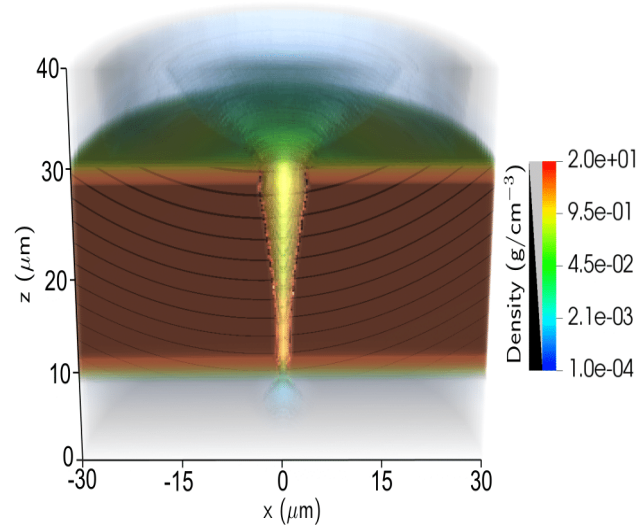


Figure 3: Simulation snapshot showing the expansion of the solid foil 2 ns after the XFEL induced volume excitation.

temperature of the plasma column along the copper foil was exponentially decayed using this factor.

The simulation was modelled using a 2D cylindrical geometry. The simulation for the case discussed above is shown in Fig. 3. An analytical treatment is necessary to obtain the exact electron temperature of the plasma column but experiments can be performed to obtain a rough estimate for it. These simulations can then be used to understand the plasma expansion dynamics. The numerical results from FLASH indicate solid target option offers better damage control, while maintaining good lasing performance. A liquid jet of copper solution requires larger pump intensities and therefore is more prone to instantaneous damage.

FUTURE STEPS

Laser ablation is a multi-spatial and temporal scale problem. While the experiment presented above investigates the very late times of the material mechanical relaxation (e.g. spallation), the hydrodynamic simulations only access the first few 10s of ns of the laser energy absorption physics in the material (e.g. via shock wave propagation and lattice deformations). Using high resolution X-ray imaging techniques at XFEL as demonstrated at the Matter in Extreme Conditions [11, 12] of LCLS, we would be able to bridge the gap by investigating the first few 100s ns of the laser/matter interaction with sub-micron and sub-ns resolution directly inside the material. Direct comparison between experimental data and simulation would be enabled, greatly improving our understanding of the laser/matter interaction regime relevant for the XLO project.

ACKNOWLEDGEMENTS

This work is supported by the U.S. Department of Energy Contract No. DE-AC02-76SF00515 and DESC0009914.

The software used in this work was developed in part by the DOE NNSA and DOE Office of Science supported Flash Center for Computational Science at the University of Chicago and the University of Rochester.

REFERENCES

- [1] A. Halavanau *et al.*, “Population inversion x-ray laser oscillator,” *Proceedings of the National Academy of Sciences*, vol. 117, no. 27, pp. 15 511–15 516, 2020, doi:10.1073/pnas.2005360117
- [2] M. Yadav *et al.*, “Optimization of the Gain Medium Delivery System for an X-Ray Laser Oscillator,” in *Proc. IPAC’21*, Campinas, Brazil, May 2021, pp. 524–527, doi:10.18429/JACoW-IPAC2021-MOPAB150
- [3] N. Majernik *et al.*, “Foiled Again: Solid-State Sample Delivery for High Repetition Rate XFELs,” presented at the 13th International Particle Accelerator Conference (IPAC’22), Bangkok, Thailand, paper THPOTK053, this conference.
- [4] B. Fryxell *et al.*, “FLASH: An adaptive mesh hydrodynamics code for modeling astrophysical thermonuclear flashes,” *The Astrophysical Journal Supplement Series*, vol. 131, no. 1, pp. 273–334, 2000, doi:10.1086/317361
- [5] P. Tzeferacos *et al.*, “Flash mhd simulations of experiments that study shock-generated magnetic fields,” *High Energy Density Physics*, vol. 17, pp. 24–31, 2015, 10th International Conference on High Energy Density Laboratory Astrophysics, doi:https://doi.org/10.1016/j.hedp.2014.11.003
- [6] I. Golovkin and J. Macfarlane, “New Prism EOS and Opacity Tables with NLTE Atomic Kinetics,” in *APS Division of Plasma Physics Meeting Abstracts*, vol. 2018, 2018, paper NP11.036, NP11.036.
- [7] M. N. Saha and A. Fowler, “On a physical theory of stellar spectra,” *Proceedings of the Royal Society of London. Series A, Containing Papers of a Mathematical and Physical Character*, vol. 99, no. 697, pp. 135–153, 1921, doi:10.1098/rspa.1921.0029
- [8] R. M. More, K. H. Warren, D. A. Young, and G. B. Zimmerman, “A new quotidian equation of state (qeos) for hot dense matter,” *The Physics of Fluids*, vol. 31, no. 10, pp. 3059–3078, 1988, doi:10.1063/1.866963
- [9] C. Orban, M. Fatenejad, and D. Q. Lamb, “Code-to-code comparison and validation of the radiation-hydrodynamics capabilities of the flash code using a laboratory astrophysical jet,” *Physics of Plasmas*, vol. 29, no. 5, p. 053 901, 2022, doi:10.1063/5.0079493
- [10] L. Spitzer, *Physics of fully ionized gases*. Courier Corporation, 2006.
- [11] B. Nagler *et al.*, “The Matter in Extreme Conditions instrument at the Linac Coherent Light Source,” *Journal of Synchrotron Radiation*, vol. 22, no. 3, pp. 520–525, 2015, doi:10.1107/S1600577515004865
- [12] S. B. Brown *et al.*, “Direct imaging of ultrafast lattice dynamics,” *Science Advances*, vol. 5, no. 3, eaau8044, 2019, doi:10.1126/sciadv.aau8044